Emergent pair symmetries in systems with poor man's Majorana modes

Jorge Cayao*
Department of Physics and Astronomy, Uppsala University, Box 516, S-751 20 Uppsala, Sweden

(Received 2 July 2024; accepted 27 August 2024; published 5 September 2024)

Few-site Kitaev chains are promising for realizing Majorana zero modes without topological protection but fully nonlocal, which are known as poor man's Majorana modes. While several signatures have already been reported both theoretically and experimentally, it still remains unknown what is the nature of superconducting correlations in the presence of poor man's Majorana modes. In this paper, we study few-site Kitaev chains and demonstrate that they host pair correlations with distinct symmetries, entirely determined by the underlying quantum numbers. In particular, we find that a two-site Kitaev chain hosts local (odd-frequency) and nonlocal (odd- and even-frequency) pair correlations, both spin polarized and highly tunable by the system parameters. Interestingly, the odd-frequency pair correlations exhibit a divergent behavior around zero frequency when the nonlocal p-wave pair potential and electron tunneling are of the same order, an effect that can be controlled by the on-site energies. Since a divergent odd-frequency pairing is directly connected to the intrinsic spatial nonlocality of Majorana zero modes in topological superconductors, the divergent odd-frequency pairing here reflects the intrinsic Majorana nonlocality of poor man's Majorana modes but without any relation to topology. Our findings could help understanding the emergent pair correlations in few-site Kitaev chains.

DOI: 10.1103/PhysRevB.110.125408

I. INTRODUCTION

Majorana zero modes (MZMs) emerge in topological superconductors as charge neutral quasiparticles [1–4] and have attracted an enormous interest because of their potential for quantum computing applications [5–8]. In one dimension, topological superconductivity with MZMs has been shown to appear in the so-called Kitaev chain [9], which consists of spin-polarized fermions with p-wave superconductivity. Although this type of superconductivity is scarce in nature [10], it was predicted to occur by combining conventional ingredients such as spin-singlet s-wave superconductivity, spin-orbit coupling, and a magnetic field [11,12]. The simplicity of this proposal has motivated several studies aiming to detect MZMs but, to date, there is no consensus on whether MZMs have been observed or not [13].

Part of the challenges is believed to be caused by the complex experimental setups [1,2], which inevitably enable the presence of other phenomena that obscures Majorana physics [13]. To mitigate some of the issues, Kitaev chains with few sites are now being pursued [14–17], thus offering a bottom-up engineering approach. In this case, MZMs emerge at fine-tuned single points in the parameter space, commonly referred to as sweet spots, but do not exhibit any topological protection [18]. For this reason, such MZMs were coined as poor man's Majorana modes (PMMMs); see also Ref. [19]. Interestingly, these PMMMs appear as charge neutral quasiparticles, having zero energy and being spatially nonlocal [20,21], in the same way as MZMs in topological superconductors [4]. A unique consequence of the charge neutrality of MZMs is that it originates a divergent odd-frequency pairing that is intimately tied to their topology [4,22–24], revealing that the superconducting pairing with MZMs is highly unusual, see also Refs. [25–35].

Under general conditions, the superconducting pairing can have even- or odd-frequency symmetries, where the paired electrons forming Cooper pairs have a pair amplitude that is *even* or *odd* in their relative time, or frequency, see e.g., Refs. [23,36]. Identifying the pair symmetries can therefore help understanding the type of emergent superconducting pairing. Since PMMMs exhibit a charge neutrality similar to MZMs but lack of topological protection [18,20,21], it is natural to wonder what is the nature of the emergent superconducting pairing in the presence of PMMMs.

In this paper, we consider a few-site Kitaev chain (Fig. 1) and investigate the emergence of superconducting pair correlations. By carrying out a full symmetry classification that

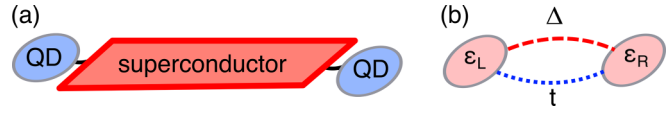

FIG. 1. (a) A superconductor with Rashba spin-orbit coupling (red) under a magnetic field is coupled to two quantum dots (QDs in blue). (b) The QDs become superconducting (light red) with a spin-polarized p-wave pair potential Δ and a hopping amplitude t, effectively realizing a two-site Kitaev chain. The on-site energies of the QDs is denoted by $\varepsilon_{L,R}$.

*Contact author: jorge.cayao@physics.uu.se

involves all the quantum numbers in these type of systems, we find that there are multiple pair symmetries naturally emerging both locally and nonlocally. In general, local superconducting pair amplitudes appear with an odd-frequency dependence, while nonlocally the pair amplitudes can exhibit even- and odd-frequency profiles. More specifically, we demonstrate in a two-site Kitaev chain that the local pair correlations develop an odd-frequency dependence with a divergent profile around zero frequency when the nonlocal p-wave pair potential and electron tunneling are equal (sweet spot) and at least one on-site energy vanishes. Furthermore, the nonlocal pair correlations also exhibit a similar divergent frequency profile but, unlike the local pairing, requires having distinct on-site energies and at least one of them vanishing. Away from the stringent sweet spot conditions, the local and nonlocal odd-frequency pair amplitudes follow a linear frequency dependence, reaching zero value at zero frequency. The divergent odd-frequency pairing reveals a behavior of the emergent superconducting correlations that is similar to what occurs in topological superconductors with MZMs but here without any relation to topology. Our findings might be useful for understanding the type of emergent superconducting correlations in few-site Kitaev chains with PMMMs.

The remainder of this paper is organized as follows. In Sec. II we discuss the allowed pair symmetries in few-site Kitaev chains. In Sec. III we present the model of a two-site Kitaev chain, discuss its spectral properties, and demonstrate the emergence of local and nonlocal superconducting pair correlations. Finally, we present our conclusions in Sec. IV,

II. PAIR SYMMETRIES IN FEW-SITE KITAEV CHAINS

We begin by providing a general symmetry classification of the superconducting pair correlations allowed by all the quantum numbers in few-site Kitaev chains. To characterize the superconducting pair correlations, we employ the anomalous Green's function defined as $\mathcal{F}^{nm}_{\alpha\beta}(t,t') = \langle \mathcal{T} c_{\alpha n}(t) c_{\beta m}(t') \rangle$ where $\mathcal{T}$ is the time ordering operator, $c_{n\alpha}(t)$ annihilates an electronic state in site α of superconductor n at time t [37,38]. The anomalous Green's function $\mathcal{F}^{nm}_{\alpha\beta}(t,t')$ is also known as pair amplitude or pair correlation and its formation is fully tied to the quantum numbers of the two paired electrons, namely, (n,m), (α,β), and time coordinates (t,t'). For instance, the spin configuration of the Kitaev chain already dictates the spin symmetry of $\mathcal{F}^{nm}_{\alpha\beta}$ since we do not assume any active spin field: the Kitaev chain consists of spin-polarized fermions [9], which implies that all the fermions have the same spin and that the pair amplitude has a spin-triplet symmetry [25–32]; see also Ref. [39].

The symmetries with respect to the other quantum numbers (n,m), (α,β), and time coordinates (t,t') are not arbitrary but must respect the fermionic nature of the composed electrons. Since the pair amplitude behaves as a two-electron wavefunction, it must fulfill the antisymmetry condition such that $\mathcal{F}^{nm}_{\alpha\beta}(t,t') = -\mathcal{F}^{mn}_{\beta\alpha}(t',t)$ under the total exchange of quantum numbers plus exchange of time coordinates [22,23,40]. Similarly, in frequency domain, the antisymmetry condition implies $F^{nm}_{\alpha\beta}(\omega) = -F^{mn}_{\beta\alpha}(-\omega)$, where $F^{nm}_{\alpha\beta}(\omega)$ is the Fourier transform of $\mathcal{F}^{nm}_{\alpha\beta}(t,t')$. Thus, the allowed pair symmetries must be antisymmetric under a total exchange of quantum numbers. Taking this into account, under the individual exchange of frequency (ω), site indices (α,β), and superconductor indices (n,m), the pair amplitude can be either an *even* (E) or *odd* (O) function. As pointed out in the previous paragraph, the Kitaev chain involves spin-polarized fermions, which leaves the spin symmetry to be triplet (T). We find that there are four distinct spin-triplet pair symmetries that obey the antisymmetry condition, see Table I. It can be seen that the superconductor index n (sup. index), as well as the dot index α, play a role that is similar to the band index in multiband superconductors [40–44] and sideband index in Floquet superconductors [45,46], see also Ref. [47]. The sup. index n becomes active when multiple few-site Kitaev chains are coupled, e.g., in Josephson junctions [48], which are expected to be useful for realizing superconducting circuits. However, by focusing on the pair amplitudes inside a given superconductor, the sup. index restricts its symmetry to be *even* and only two pair symmetry classes are allowed: even-frequency, spin-triplet, odd under dot index, even under sup. index or ETOE; odd-frequency, spin-triplet, even under dot index, even under sup. index or OTEE. While in general all the allowed pair symmetries can appear as a linear combination, and can therefore coexist, the dominance of a particular symmetry characterizes the type of emergent superconducting pairing. Therefore, under general circumstances, few-site Kitaev chains are expected to host distinct types of pair symmetry classes.

TABLE I. Allowed superconducting pair symmetries in few-site Kitaev chains as a result of the total antisymmetrization of the pair amplitudes when exchanging frequency, spins, site index, and superconducting (sup.) index. In a two-site Kitaev chain, which involves a single superconducting system, only ETOE and OTEE classes are present.

Frequency $(\omega \leftrightarrow -\omega)$	Spin $(\uparrow\leftrightarrow\downarrow)$	Site index $(\alpha \leftrightarrow \beta)$	Sup. index $(n \leftrightarrow m)$	Class (total exchange)
Even	Triplet	Even	Odd	ETEO
Even	Triplet	Odd	Even	ETOE
Odd	Triplet	Even	Even	OTEE
Odd	Triplet	Odd	Odd	OTOO

III. EMERGENT PAIR CORRELATIONS IN TWO-SITE KITAEV CHAINS

Having discussed the allowed pair symmetries in few-site Kitaev chains, we now explore their formation in a two-site Kitaev chain, which consists of two spin-polarized coupled sites with p-wave pairing, see Fig. 1(b). In the basis $\Psi = (c_L, c_R, c_L^\dagger, c_R^\dagger)$, the two-site Kitaev chain is modelled by the following Bogoliubov-de Gennes (BdG) Hamiltonian:

$$H_{\mathrm{BdG}} = \varepsilon_L \eta_+ \tau_z + \varepsilon_R \eta_- \tau_z + t \eta_x \tau_z - \Delta \eta_y \tau_y, \qquad (1)$$

where ε_α is the on-site energy of dot $\alpha = L/R$, t is the hopping amplitude, and Δ the p-wave pair potential. Moreover, $\eta_\pm = (\eta_0 \pm \eta_z)/2$, with η_i the ith Pauli matrix in the site subspace, while τ_i the Pauli matrix in Nambu subspace.

Notably, the minimal Kitaev chain given by Eq. (1) at the sweet spot $\varepsilon_{L,R} = 0$ and $\Delta = t$ hosts a pair of MZMs, with their wavefunctions fully located at the left and right sites but without being topologically protected, namely, Eq. (1) hosts a pair of PMMMs [18]. Moreover, it is worth noting that two-site Kitaev chain also holds experimental relevance as it has been recently realized in superconductor-semiconductor hybrids [14], see Fig. 1(a). Most of the properties of PMMMs have been shown to be similar to those of MZMs in topological superconductors. However, the nature of the induce superconducting pairing is still unknown. In particular, being the PMMMs of Majorana origin and having an intrinsic charge neutrality poses the question about the type of induced superconducting pairing.

We are here interested in the emergent pair symmetries under the presence of PMMMs, which, as discussed in Sec. III, requires the calculation of the anomalous electron-hole Green's function. For this purpose, we obtain the Green's function of the BdG Hamiltonian given by Eq. (1),

$$\mathcal{G}(\omega) = \begin{pmatrix} G(\omega) & F(\omega) \\ \bar{F}(\omega) & \bar{G}(\omega) \end{pmatrix} = (\omega - H_{\rm BdG})^{-1}, \tag{2}$$

where ω represents complex frequencies unless otherwise specified. Here, the diagonal components (G and $\bar{G}$) represent the normal electron-electron and hole-hole Green's functions, while (F and $\bar{F}$) are the anomalous electron-hole and hole-electron Green's functions. Note that the normal and anomalous Green's functions are still matrices in the subspace spanned by the two sites, see also Eq. (1). While G enables the calculation of the spectral function, F determines the superconducting pairing. For completeness, in what follows we explore first the spectral function and then focus on the emergent pair symmetries.

A. Majorana signatures in the spectral function

Before addressing the pair correlations, it is worth discussing the formation of PMMMs. While this can be carried out in different ways, it is useful to explore the spectral function not only because it can be directly obtained from the normal Green's functions obtained above but, importantly, also because it can be experimentally accessed via conductance measurements [49]. Since conductance is often measured in Majorana experiments [13,14], the spectral signatures of PMMMs can help understanding their formation. By using Eqs. (1) and (2), we find the normal Green's function components given by

$$\begin{aligned} G_{\rm LL}(\omega) &= \frac{t^2(\varepsilon_{\rm R} - \omega) - (\varepsilon_{\rm R} + \omega)P_{\rm LR}(\omega)}{D(\omega)}, \\ G_{\rm RR}(\omega) &= \frac{t^2(\varepsilon_{\rm L} - \omega) - (\varepsilon_{\rm L} + \omega)P_{\rm RL}(\omega)}{D(\omega)}, \\ G_{\rm LR}(\omega) &= \frac{t[\Delta^2 - t^2 + (\varepsilon_{\rm L} + \omega)(\varepsilon_{\rm R} + \omega)]}{D(\omega)}, \\ G_{\rm RL}(\omega) &= G_{\rm LR}(\omega), \end{aligned} \tag{3}$$

where $P_{\rm LR(RL)}(\omega) = [\Delta^2 + (\varepsilon_{\rm L(R)} + \omega)(\varepsilon_{\rm R(L)} - \omega)]$ and $D(\omega) = (\Delta^2 - t^2 + \varepsilon_{\rm L}\varepsilon_{\rm R})^2 - (2t^2 + 2\Delta^2 + \varepsilon_{\rm L}^2 + \varepsilon_{\rm R}^2)\omega^2 + \omega^4$. Also, $\bar{G}_{\rm LL(RR)} = G_{\rm LL(RR)}(\varepsilon_\alpha \to -\varepsilon_\alpha)$, $\bar{G}_{\rm LR(RL)} = -G_{\rm LR(RL)}(\varepsilon_\alpha \to -\varepsilon_\alpha)$. For simplicity but without loss of generality we focus on the spectral function in the left site obtained as $A_{\rm L}^e(\omega) = -{\rm Im}{\rm Tr}G_{\rm LL}(\omega + i\eta)$ where η is an infinitesimal positive number enabling the analytic continuation to real frequencies ω [37]. To access $A_{\rm L}^e$ via conductance, the left site of the two-site Kitaev chain can be coupled to a normal lead [49,50]. In Fig. 2 we present $A_{\rm L}^e(\omega)$ as a function of real frequency ω and on-site energies $\varepsilon_{\rm L,R}$. The top and bottom rows correspond to the spectral function at sweet spot $\Delta = t$ and away from it $\Delta \neq t$. The immediate feature we observe is that the spectral function reveals the energy levels of the two-site Kitaev chain [18], which read $E_\pm^s = \pm|\sqrt{t^2 + \varepsilon_-^2} - (-1)^s\sqrt{\Delta^2 + \varepsilon_+^2}|$, where $\varepsilon_\pm = (\varepsilon_{\rm L} \pm \varepsilon_{\rm R})/2$ and $s = 0$ ($s = 1$) labels the two lowest (excited) levels. The features of the energy levels in spectral function is of course expected because the poles of the Green's function $G_{\rm LL}$ are directly connected to the spectrum of $H_{\rm BdG}$, see Eq. (2).

In the sweet spot $\Delta = t$, when one of the on-site energies vanishes, the spectral function $A_{\rm L}^e(\omega)$ develops a large value at zero frequency, as seen in Fig. 2(a). This can be understood by noting that $G_{\rm LL}(\omega)$ given in Eqs. (3) develops a zero-frequency resonance at $\varepsilon_{\rm R} = 0$ and $\Delta = t$, namely, $G_{\rm LL}(\omega) = [\omega(\omega + \varepsilon_{\rm L}) - 2\Delta^2]/\{\omega[\omega^2 - (4\Delta^2 + \varepsilon_{\rm L}^2)]\}$; the zero-frequency resonance is then evident from the $1/\omega$ dependence of $G_{\rm LL}$. This zero-frequency resonance corresponds to having $E_\pm^0 = 0$ at $\Delta = t$ and $\varepsilon_{\rm R} = 0$, which corresponds to the energy of PMMMs [18]. By inducing a finite on-site energy in the right dot, the spectral function develops a bowtie-like profile around zero frequency and acquires large zero-frequency values only when the left on-site energy vanishes, as seen in Fig. 2(b). Similarly, in the case of having equal on-site energies, the spectral function becomes large at zero frequency only when such energies vanish, see Fig. 2(c). We can therefore conclude that the emergence of PMMMs is reflected in large zero-frequency values of the spectral function.

Away from the sweet spot condition, when $\Delta \neq t$, the situation becomes drastically different, see Figs. 2(d)–2(f). In this case, when one of the on-site energies is fixed at zero, the spectral function acquires a diamond-like profile around zero frequency but does not reach large zero-frequency values, see Fig. 2(d). A finite right on-site energy then leads to an asymmetric profile with respect $\varepsilon_{\rm R} = 0$, inducing a large zero-frequency spectral weight at $\varepsilon_{\rm L} = (t^2 - \Delta^2)/\varepsilon_{\rm R}$. For equal on-site energies $\varepsilon_{\rm L,R} = \varepsilon$, the spectral function exhibits large zero-frequency values at $\varepsilon = \pm\sqrt{t^2 - \Delta^2}$, as observed in Fig. 2(f). Away from the sweet spot $\Delta \neq t$, however, no PMMMs exist [18]. Only at the sweet spot stable zero-energy states appear with large spectral weights.

B. Emergent pair amplitudes

We now explore the symmetries of the emergent pair amplitudes, which we obtain from the anomalous Green's functions. By using Eqs. (1) and (2), we find that the anomalous

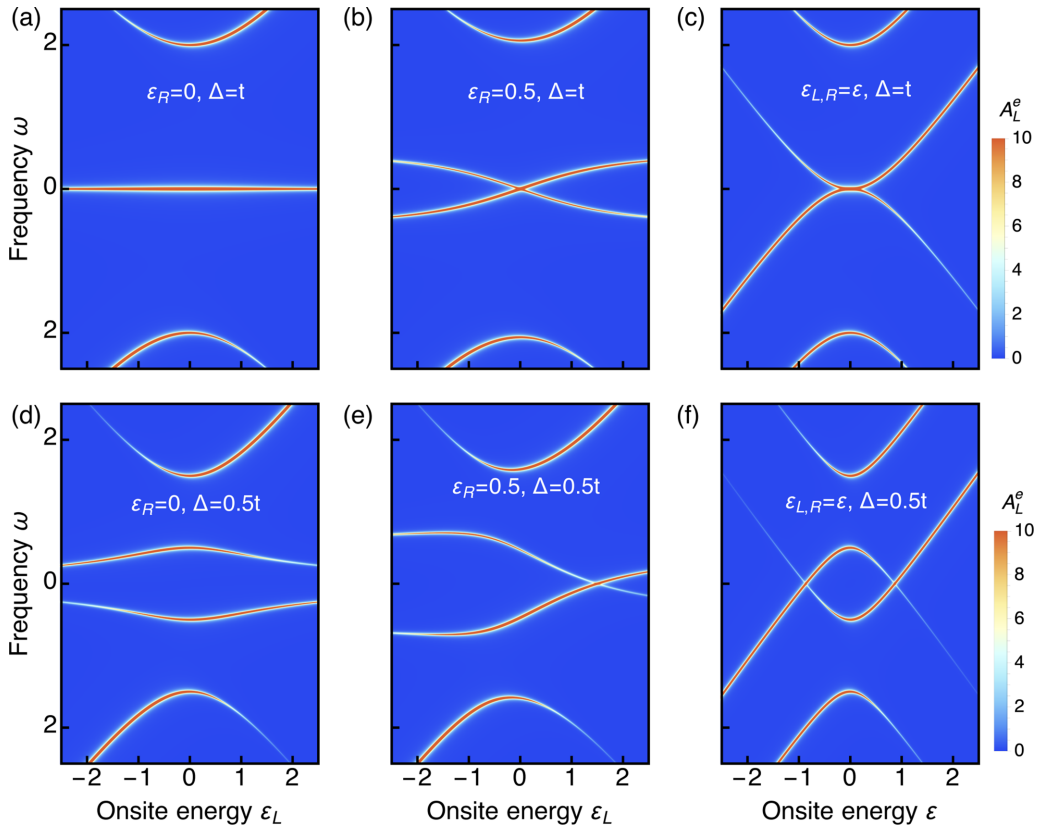

FIG. 2. Spectral function in the left dot $A_{\rm L}^e$ as a function of frequency ω and on-site energies. Panels (a)–(c) correspond to $\Delta = t$ with $\varepsilon_{\rm R} = 0$, $\varepsilon_{\rm R} = 0.5$, $\varepsilon_{\rm L,R} = \varepsilon$. Panels (d)–(f) the same as in (a)–(c) but at $\Delta = 0.5t$.

Green's function components are given by

$$
\begin{aligned}
F_{\rm LL}(\omega) &= \frac{2\omega t\,\Delta}{D(\omega)},\\
F_{\rm RR}(\omega) &= -\frac{2\omega t\,\Delta}{D(\omega)},\\
F^{+}_{\rm LR}(\omega) &= \frac{\omega(\varepsilon_{\rm R}-\varepsilon_{\rm L})\Delta}{D(\omega)},\\
F^{-}_{\rm LR}(\omega) &= \frac{\Delta(\Delta^2 - t^2 + \varepsilon_{\rm L}\varepsilon_{\rm R} - \omega^2)}{D(\omega)},
\end{aligned}
\tag{4}
$$

where ω represents complex frequencies, $F^{\pm}_{\rm LR} = (F_{\rm LR} \pm F_{\rm RL})/2$, and $D(\omega)$ is given below Eq. (3). Moreover, $\bar{F}_{\rm LL(RR)} = F_{\rm LL(RR)}(\varepsilon_\alpha \to -\varepsilon_\alpha)$ and $\bar{F}^{\pm}_{\rm LR(RL)} = -F^{\pm}_{\rm LR(RL)}(\varepsilon_\alpha \to -\varepsilon_\alpha)$. Equations (4) represent the emergent superconducting pair amplitudes in a two-site Kitaev chain, which puts us in position to identify their symmetries following Sec. III. As discussed in Sec. III, the pair symmetries depend on the quantum numbers associated to the site indices, sup. indices, spins, and frequency. Since here we consider a single superconducting system, the pair amplitudes can only be *even* under the exchange of such a sup. index. Moreover, since we deal with spinless fermions, the pair amplitudes have a *spin-triplet* symmetry, see Sec. III. Thus, all the pair amplitudes in Eqs. (4) are *spin-triplet* and *even* in the sup. index. The remaining symmetries, with respect to the site indices and frequency, however, are not the same for all the pair amplitudes in Eqs. (4) and, as we will see below, will determine the type of emergent superconducting pairings.

Locally, the on-site pair amplitudes $F_{\rm LL(RR)}$ are evidently *even* under the exchange of the site index $\alpha = L, R$ and *odd* functions of frequency ω; note that $D(\omega) = D(-\omega)$ is an even function of ω and $F_{\rm LL(RR)}$ exhibit opposite sign [51]. Thus, the local pair amplitudes exhibit an odd-frequency, spin-triplet, even-site, even-sup. symmetry, which corresponds to the symmetry class OTEE of Table I. This pair symmetry class is the only type of local emergent superconducting pairing emerging in these type of systems; note that the two-site Kitaev chain does not have a local superconducting pair potential, revealing that the OTEE class is indeed an emergent superconducting pairing. When it comes to the nonlocal pair amplitudes $F^{\pm}_{\rm LR}$, the expressions given in Eqs. (4) are already symmetrized with respect to the site index: $F^{+}_{\rm LR}$ is *even* under the exchange of L and R, while $F^{-}_{\rm LR}$ is *odd*. Moreover, Eqs. (4) already reveal that $F^{+}_{\rm LR}$ and is an *odd* function of ω while $F^{-}_{\rm LR}$ is an *even* function of ω. With these considerations, together with the *spin-triplet* and *even*-sup. index symmetries, it is already clear that $F^{+}_{\rm LR}$ and $F^{-}_{\rm LR}$ correspond to the OTEE and ETOE symmetry classes of Table I. Thus, nonlocally, the two-site Kitaev chain hosts two types of superconducting correlations, with the OTEE being entirely induced while the ETOE pairing tied to the parent p-wave pair potential.

Therefore, two-site Kitaev chains host two types of superconducting pairing, OTEE locally while OTEE and ETOE nonlocally, provided the parent superconductor is spin polarized and p wave. It is now necessary to inspect the behavior

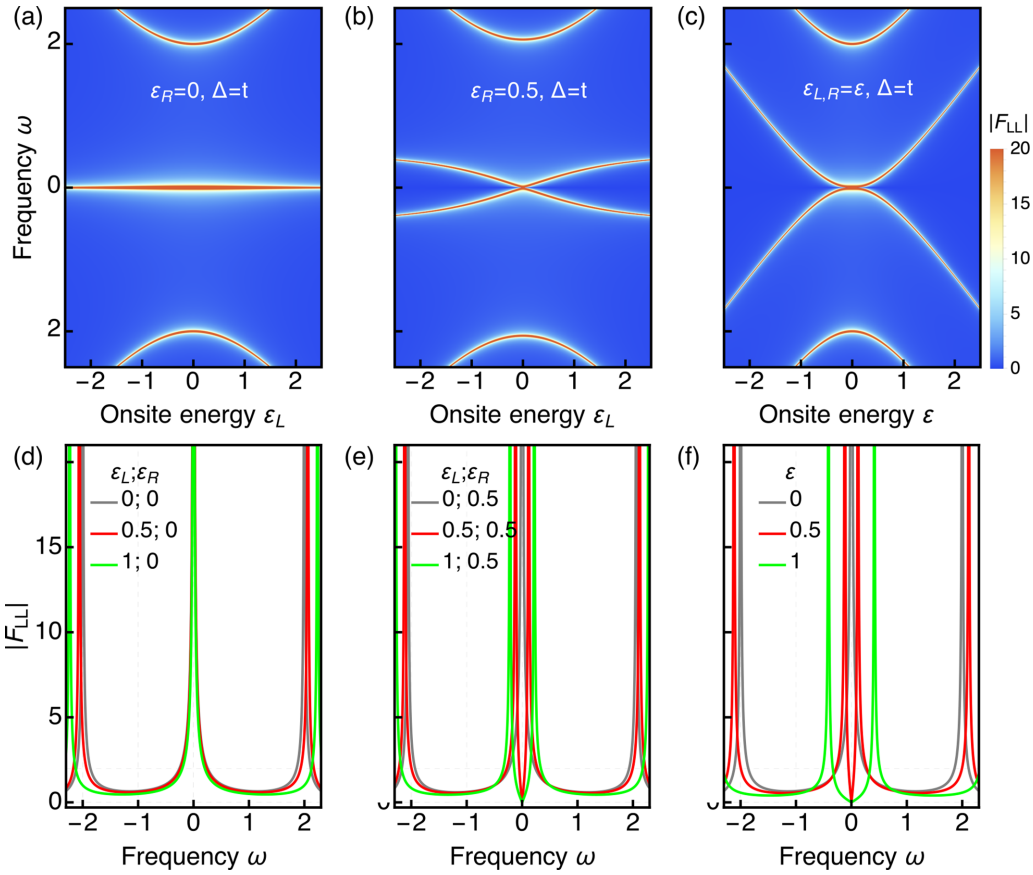

FIG. 3. (a)–(c) Absolute value of the local pair amplitude in the left dot $|F_{\rm LL}|$ as a function of frequency ω and on-site energy $\varepsilon_{\rm L}$ at $\Delta = t$ and $\varepsilon_{\rm R} = 0, 0.5, \varepsilon_{\rm L}$. (d)–(f) $|F_{\rm LL}|$ as a function of ω at distinct $\varepsilon_{\rm L,R}$.

of these emergent pair correlations as a function of the system parameters and contrast their presence under the presence and absence of PMMMs.

C. Pair amplitudes at the sweet spot $\Delta = t$

In the sweet spot regime $\Delta = t$, but still maintaining finite on-site energies, the pair amplitudes given by Eqs. (4) are given by

$$
\begin{aligned}
F_{\rm LL}(\omega) &= \frac{2\omega t^2}{\omega^4 - \left(4t^2 + \varepsilon_{\rm L}^2 + \varepsilon_{\rm R}^2\right)\omega^2 + \varepsilon_{\rm L}^2\varepsilon_{\rm R}^2}, \\
F_{\rm RR}(\omega) &= -\frac{2\omega t^2}{\omega^4 - \left(4t^2 + \varepsilon_{\rm L}^2 + \varepsilon_{\rm R}^2\right)\omega^2 + \varepsilon_{\rm L}^2\varepsilon_{\rm R}^2}, \\
F_{\rm LR}^{+}(\omega) &= \frac{\omega(\varepsilon_{\rm R} - \varepsilon_{\rm L})t}{\omega^4 - \left(4t^2 + \varepsilon_{\rm L}^2 + \varepsilon_{\rm R}^2\right)\omega^2 + \varepsilon_{\rm L}^2\varepsilon_{\rm R}^2}, \\
F_{\rm RL}^{-}(\omega) &= \frac{(\varepsilon_{\rm L}\varepsilon_{\rm R} - \omega^2)t}{\omega^4 - \left(4t^2 + \varepsilon_{\rm L}^2 + \varepsilon_{\rm R}^2\right)\omega^2 + \varepsilon_{\rm L}^2\varepsilon_{\rm R}^2}.
\end{aligned} \tag{5}
$$

To visualize the behavior of these pair amplitudes, in Figs. 3 and 4 we plot the absolute value of the local ($F_{\rm LL}$) and nonlocal ($F_{\rm LR}^{\pm}$) amplitudes in the sweet spot $\Delta = t$. In both cases we show the pair amplitudes as a function of frequency ω and on-site energies $\varepsilon_{\rm L,R}$ [Figs. 3(a)–3(c) and Figs. 4(a), 4(b), 4(e), and 4(f)] and also the sole frequency dependence at fixed $\varepsilon_{\rm L,R}$ [Figs. 3(d)–3(f) and Figs. 4(c), 4(d), 4(g), and 4(h)]. The first feature we identify is that the pair amplitudes reveal the formation of the energy levels discussed in the spectral function in the previous subsection, expected because both quantities share the same denominator, see Eqs. (4) [and also Eqs. (3) and (5)]. The numerators of Eqs. (4) develop some interesting dependencies purely associated to the type of emergent pair correlation.

In the case of the local pair amplitudes $F_{\rm LL/RR}$, when one of the on-site energy vanishes (e.g., $\varepsilon_{\rm R} = 0$), we find that they acquire large zero-frequency values irrespective of the finite value of the other on-site energy (e.g., $\varepsilon_{\rm L}$), see Fig. 3(a) for $|F_{\rm LL}|$. By inspecting the frequency dependence of $|F_{\rm LL}|$ at $\varepsilon_{\rm R} = 0$ and different $\varepsilon_{\rm L}$ in Fig. 3(d), we observe that $|F_{\rm LL}|$ has a divergent profile around $\omega = 0$ irrespective of the value of $\varepsilon_{\rm L}$; see also gray curves in Figs. 3(e) and 3(f). To understand this intriguing divergent frequency dependence, we write down the local pair amplitudes given by Eqs. (5) at $\varepsilon_{\rm R} = 0$, obtaining

$$
\begin{aligned}
F_{\rm LL}(\omega) &= \frac{1}{\omega}\left[\frac{2t^2}{\omega^2 - \left(4t^2 + \varepsilon_{\rm L}^2\right)}\right], \\
F_{\rm RR}(\omega) &= -\frac{1}{\omega}\left[\frac{2t^2}{\omega^2 - \left(4t^2 + \varepsilon_{\rm L}^2\right)}\right],
\end{aligned} \tag{6}
$$

which at low frequencies can be approximated by $F_{\rm LL/RR}(\omega) \approx \mp[1/(2\omega)] \mp [\omega/(8\Delta)]$. It is thus evident the emergence of local pair amplitudes with a divergent

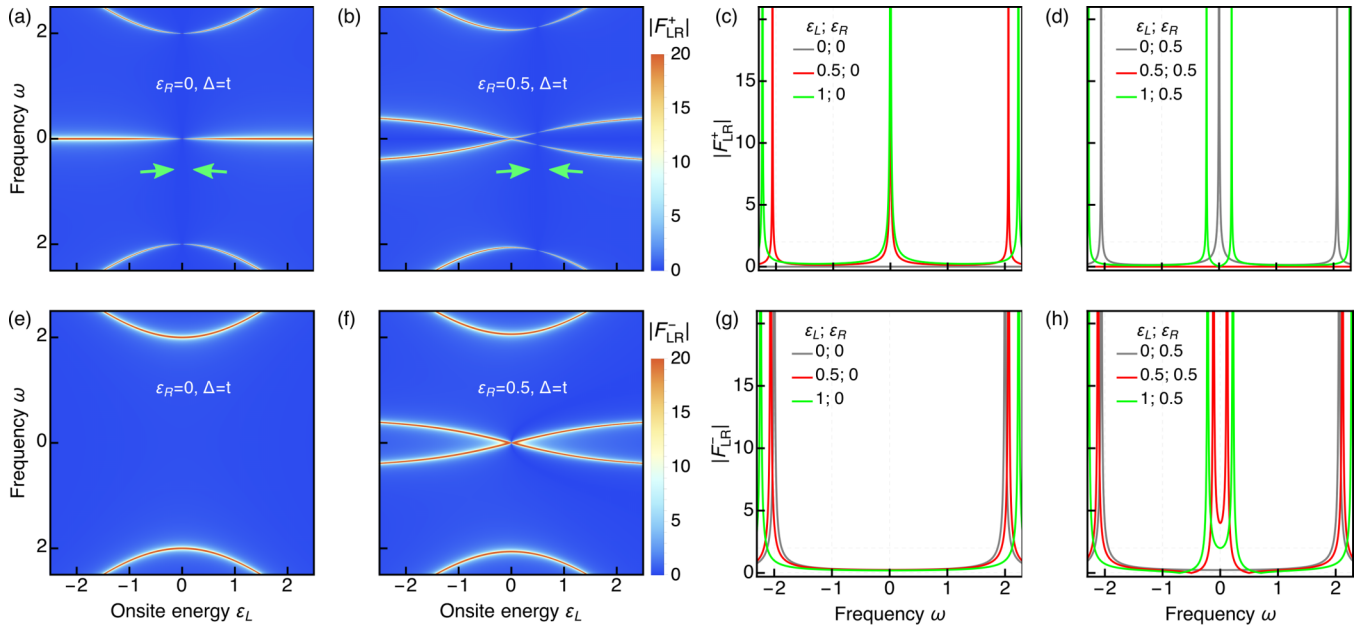

FIG. 4. (a), (b) Absolute value of the nonlocal pair amplitudes $|F^+_{\mathrm{LR}}|$ as a function of frequency ω and on-site energy ε_{L} at $\Delta = t$ and $\varepsilon_{\mathrm{R}} = 0, 0.5$. (c), (d) $|F^+_{\mathrm{LR}}|$ as a function of ω at distinct values of $\varepsilon_{\mathrm{L,R}}$. (e)–(h) Same as (a)–(d) but for $|F^-_{\mathrm{LR}}|$.

profile near zero frequency [Figs. 3(a) and 3(d)]. Since the local pair amplitudes correspond to the OTEE pair symmetry class, their odd-frequency symmetry is fully determined by having a divergent frequency dependence. As noted in the Introduction, having divergent odd-frequency pair amplitudes is a unique property of topological superconductors with MZMs, associated to topology and revealing the Majorana nonlocality [25–32]; see also Refs. [4,22–24]. In the present case, however, our minimal two-site Kitaev chain in the sweet spot hosts PMMMs without any topological properties, but, surprisingly, we find divergent odd-frequency pairing. This occurs because even in the two-site Kitaev chain, it is possible to realize a pair of fully nonlocal zero-energy PMMMs in the same way as MZMs. The relation between Majorana nonlocality and divergent odd-frequency pairing can be further understood by noting that Majorana operators fulfill a self-conjugation property $\gamma_i^\dagger = \gamma_i$, which occurs when MZMs are fully nonlocal and charge neutral [4], namely, well separated from each other without any energy splitting and spatial overlap between them. Thus, taking into account $\gamma_i^\dagger = \gamma_i$, the anomalous pair correlation (f) of a Majorana operator can be written as $f \sim \langle \gamma_i \gamma_i^\dagger \rangle = \langle \gamma_i \gamma_i \rangle = 1/\omega$. Thus, the Majorana nonlocality, inherited by both MZMs in topological superconductors and PMMMs in few-site Kitaev chains, naturally produce a divergent odd-frequency pairing as a strong signature of their unusual superconducting pairing.

The large values of $|F_{\mathrm{LL}}|$ are also seen when $\varepsilon_{\mathrm{R}} \neq 0$ in Figs. 3(b) and 3(e), where the local pair amplitude forms a divergent profile near zero frequency only when $\varepsilon_{\mathrm{L}} = 0$, consistent with the discussion presented in the previous paragraph. A similar behavior occurs when both on-site energies are equal in Figs. 3(c) and 3(f), giving rise to divergent values of $|F_{\mathrm{LL}}|$ only when both energies vanish. Thus, having both on-site energies with finite values results in local pair amplitudes that vanish at $\omega = 0$, which occurs because in this case there is a linear frequency dependence in the numerator of Eqs. (5); hence, the local pair amplitudes approach linearly to zero frequency. This behavior is observed in red and green curves of Figs. 3(e) and 3(f), supporting the idea that the divergent frequency behavior is a unique property of the sweet spot regime with $\Delta = t$ and vanishing values of either of the on-site energies.

For the nonlocal pair amplitudes $F^{\pm}_{\mathrm{LR}}$, both correspond to distinct pair symmetries and this is reflected in Figs. 4(a)–4(d) and Figs. 4(e)–4(h) for the OTEE F^+_{LR} and ETOE pair symmetry classes, respectively. To understand this behavior we write down $F^{\pm}_{\mathrm{LR}}$ from Eqs. (5) at $\varepsilon_{\mathrm{R}} = 0$ and obtain

$$F^+_{\mathrm{LR}}(\omega) = -\frac{1}{\omega}\left[\frac{\varepsilon_{\mathrm{L}} t}{\omega^2 - \left(4t^2 + \varepsilon_{\mathrm{L}}^2\right)}\right],$$
$$F^-_{\mathrm{RL}}(\omega) = -\left[\frac{t}{\omega^2 - \left(4t^2 + \varepsilon_{\mathrm{L}}^2\right)}\right]. \tag{7}$$

Thus, at vanishing one on-site energy (e.g., $\varepsilon_{\mathrm{R}} = 0$), the OTEE class $|F^+_{\mathrm{LR}}|$ exhibits large values at zero frequency as a function of ε_{L} but vanishes at $\varepsilon_{\mathrm{L}} = 0$, see Fig. 4(a) and the green arrows; see also gray curve in Fig. 4(c). The large zero-frequency values of $|F^+_{\mathrm{LR}}|$ remain robust under variations of $\varepsilon_{\mathrm{L}} \neq 0$, provided $\varepsilon_{\mathrm{R}} = 0$; for $\varepsilon_{\mathrm{R}} \neq 0$, $|F^+_{\mathrm{LR}}|$ gets large values only near $\omega = 0$, see also Fig. 4(b). Thus, when one of the on-site energies is finite and the other vanishes, $|F^+_{\mathrm{LR}}|$ develops a divergent profile near zero frequency, see red and green curves in Fig. 4(c) and also gray curve in Fig. 4(d). This divergent profile is similar to what we found for the local pair amplitude discussed in previous subsection and can be understood to be a consequence of the Majorana nonlocality. This stems from the fact that, given distinct Majorana operators, obeying the self-conjugation Majorana property because of Majorana nonlocality, a pair correlation between two of them still yields a divergent odd-frequency nonlocal pairing, in the same way as it happens for the local pair amplitudes in Eqs. (6). Thus,

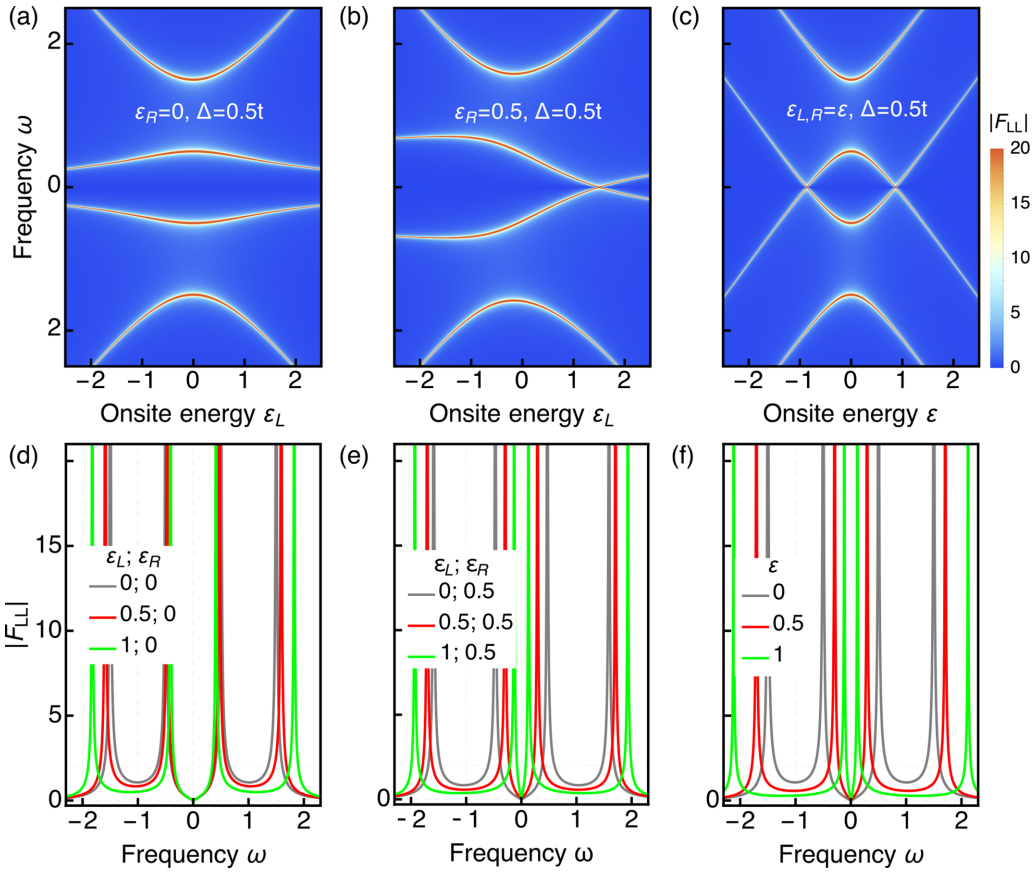

FIG. 5. (a)–(c) Absolute value of the local pair amplitude in the left dot $|F_{\rm LL}|$ as a function of frequency ω and on-site energy $\varepsilon_{\rm L}$ at $\Delta = 0.5t$ and $\varepsilon_{\rm R} = 0, 0.5, \varepsilon_{\rm L}$. (d)–(f) $|F_{\rm LL}|$ as a function of ω at distinct $\varepsilon_{\rm L,R}$.

having $F^{+}_{\rm LR}$ as a divergent odd-frequency nonlocal pairing in the presence of PMMMs can be interpreted as a measure of Majorana nonlocality. For finite on-site energies, however, no divergent profile is obtained: $|F^{+}_{\rm LR}|$ is peaked at the frequencies of the energy levels occurring away from zero frequency and vanish at $\varepsilon_{\rm R} = \varepsilon_{\rm L}$, see green arrows in Fig. 4(b) and red curve in Fig. 4(d). Away from this vanishing value but at distinct on-site energies, we find $|F^{+}_{\rm LR}|$ to depend linearly on ω when approaching zero frequency, see green curve in Fig. 4(d) and third expression in Eqs. (5).

In contrast to the behavior of the nonlocal OTEE pairing $F^{+}_{\rm LR}$, the nonlocal ETOE pair amplitude $F^{-}_{\rm LR}$ does not vanish at any on-site energy and does exhibit any divergent profile at zero frequency even at vanishing on-site energies, see Figs. 4(e) and 4(g). This behavior directly follows Eq. (7), which shows that $F^{-}_{\rm LR}$ only captures the gap edges when either (or both) of the on-site energies vanish. At finite on-site energies, $|F^{-}_{\rm LR}|$ has a dip near zero frequency, whose minimum value at $\omega = 0$ reaches $|F^{-}_{\rm LR}| = |t|/|\varepsilon_{\rm L}\varepsilon_{\rm R}|$, see Eq. (5).

We have therefore obtained that two-site Kitaev chains in the sweet spot $\Delta = t$ exhibit local OTEE pair amplitudes with a divergent odd-frequency dependence around zero frequency, provided one or both on-site energies vanish. Moreover, the nonlocal OTEE pair symmetry class also exhibits a divergent odd-frequency dependence around zero frequency, as long as either of the on-site energies vanishes and $\varepsilon_{\rm L} \neq \varepsilon_{\rm R}$. Thus, the divergent odd-frequency profile of the emergent local and nonlocal pair correlations constitute a characteristic of the unconventional superconducting state with PMMMs. It is worth noting that local and nonlocal pair correlations are expected to play an important role in local and nonlocal transport [52,53], which happens when attaching leads to the left and right sides of the two-site Kitaev chain studied here. In particular, Andreev reflection and crossed Andreev reflections can be directly determined from the local and nonlocal squared pair amplitudes [52,53], respectively. In this regard, having local and nonlocal pair correlations with distinct functionalities, as we obtain here in the presence of PMMMs, is expected to induce distinct conductance signatures that would allow to identify the type of dominant superconducting pairing.

D. Pair amplitudes away from the sweet spot $\Delta \neq t$

To inspect the behavior of the emergent pair amplitudes at $\Delta \neq t$, we directly plot Eqs. (4) in Figs. 5 and 6 for the local and nonlocal components, respectively. In Figs. 5(a)–5(c) and Figs. 6(a), 6(b), 6(e), and 6(f) we show the absolute value of the pair amplitudes $|F_{\rm LL}|$ and $|F^{\pm}_{\rm LR}|$ in the $\omega - \varepsilon_{\rm L}$ plane at $\varepsilon_{\rm R} = 0, 0.5, \varepsilon_{\rm L}$. Moreover, Figs. 5(d)–5(f) and Figs. 6(a), 6(b), 6(e), and 6(f) we present the frequency dependence of $|F_{\rm LL}|$ and $|F^{\pm}_{\rm LR}|$ at fixed values of $\varepsilon_{\rm L,R}$. The first and general observation in both the local and nonlocal pair amplitudes is that they reveal the energy levels seen in the spectral function in Figs. 2(d)–2(f). There exist, however, slight differences between the local and nonlocal pair amplitudes, which

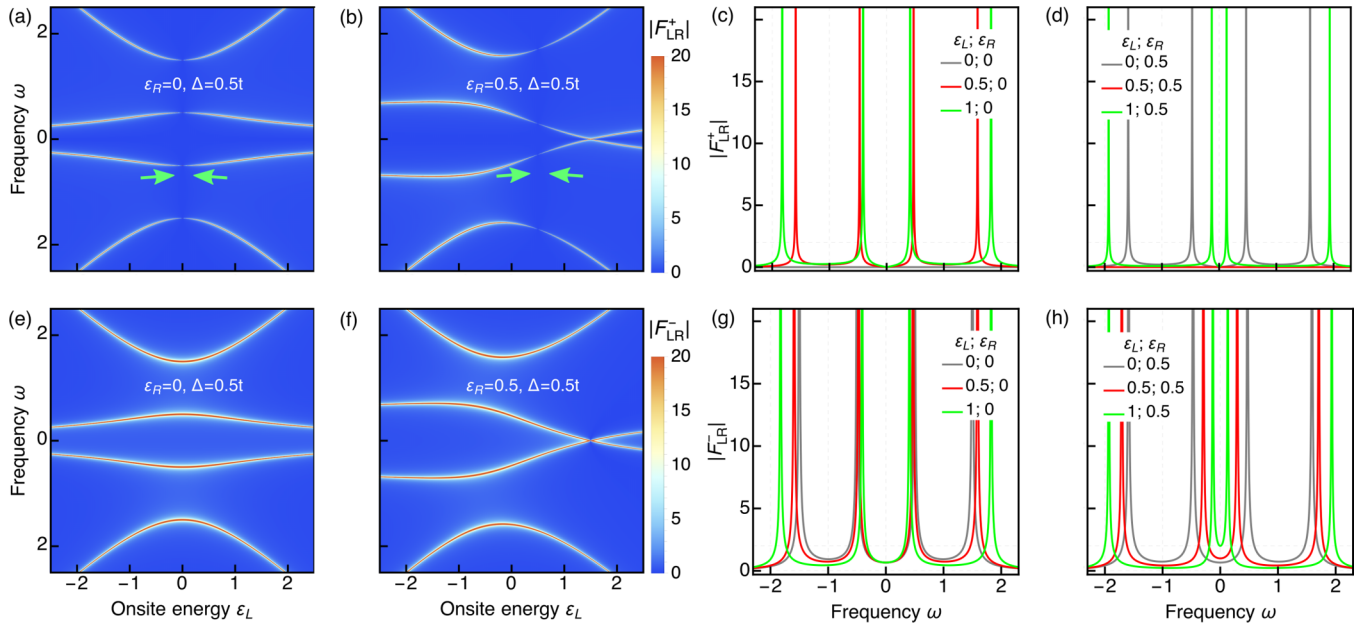

FIG. 6. (a), (b) Absolute value of the nonlocal pair amplitudes $|F^+_{\rm LR}|$ as a function of frequency ω and on-site energy $\varepsilon_{\rm L}$ at $\Delta = 0.5t$ and $\varepsilon_{\rm R} = 0, 0.5$. (c), (d) $|F^+_{\rm LR}|$ as a function of ω at distinct values of $\varepsilon_{\rm L,R}$. (e)–(h) Same as (a)–(d) but for $|F^-_{\rm LR}|$.

stems from their particular dependence on the system parameters since both belong to distinct pair symmetry classes, see Sec. III B and also Sec. III and Table I.

The local pair amplitudes, which have OTEE symmetry, vanish at zero frequency irrespective of the value of the on-site energies $\varepsilon_{\rm L,R}$, as observed in Fig. 5 for $|F_{\rm LL}|$; the same occurs for $|F_{\rm RR}|$. A close inspection reveals that $|F_{\rm LL}|$ approaches zero frequency linearly [Figs. 5(d)–5(f)], which is dramatically different to the divergent frequency profile around zero frequency at the sweet spot $\Delta = t$, see Figs. 3(a) and 3(d). Expanding the first and second expressions of Eqs. (4) at $\omega = 0$, and taking only the first order, we obtain $F_{\rm LL/RR} \approx \pm(2t\Delta\omega)/(\Delta^2 - t^2 + \varepsilon_{\rm L}\varepsilon_{\rm R})^2$, confirming the linear frequency dependence at low frequencies. Moreover, to contrast the divergent and linear frequency dependencies of the local pair amplitudes at (away from) the sweet spot $\Delta = t$, it is worth expanding them around $t = \Delta$. Keeping the first order and $\varepsilon_{\rm L,R} = 0$, we obtain

$$F_{\rm LL/RR}(t = \Delta) \approx \pm\frac{2\Delta^2}{\omega(\omega^2 - 4\Delta^2)} \pm \frac{2\omega(t - \Delta)\Delta}{\omega(\omega^2 - 4\Delta^2)^2}. \quad (8)$$

The first term clearly shows the divergent frequency dependence when approaching zero frequency at the sweet spot $t = \Delta$, while the second term reveals that deviations from $t = \Delta$ produces a linear in frequency contribution to the local pair amplitudes.

For the nonlocal pair amplitudes $|F^{\pm}_{\rm LR}|$, which posses OTEE and ETOE symmetries, respectively, we find that the OTEE pair amplitude $|F^+_{\rm LR}|$ vanishes either at zero frequency or when the on-site energies are equal $\varepsilon_{\rm L} = \varepsilon_{\rm R}$. The vanishing OTEE pair amplitude ($|F^+_{\rm LR}| = 0$) can be seen in Figs. 6(a) and 6(b) and in the gray and red curves of Figs. 6(c) and 6(d); see also green arrows in Figs. 6(a) and 6(b) indicating $|F^+_{\rm LR}| = 0$ at equal on-site energies. To understand how $|F^+_{\rm LR}|$ vanishes, it is useful to expand it at $\omega = 0$ and, keeping the first order, we find $F^+_{\rm LR} \approx \pm(\omega(\varepsilon_{\rm R} - \varepsilon_{\rm L})\Delta)/(\Delta^2 - t^2 + \varepsilon_{\rm L}\varepsilon_{\rm R})^2$; this expression also reveals that $|F^+_{\rm LR}|$ vanishes in a linear fashion when approaching zero frequency, as indeed seen in Figs. 6(c) and 6(d). In contrast to the OTEE pair class, the ETOE pair amplitude $|F^-_{\rm LR}|$ remains finite at zero frequency and when both on-site energies are equal, see Figs. 6(e)–6(h). It can only vanish when $\omega^2 = \Delta^2 - t^2 + \varepsilon_{\rm L}\varepsilon_{\rm R}$, as seen in Eqs. (4). This is, however, a very stringent condition and the $|F^-_{\rm LR}|$ can be thus expected to be in general finite. In fact, by expanding $F^-_{\rm LR}$ at zero frequency and keeping the first order, we obtain $F^-_{\rm LR} \approx \Delta/(\Delta^2 - t^2 + \varepsilon_{\rm L}\varepsilon_{\rm R})$, thus demonstrating that $F^-_{\rm LR}$ remains finite even at zero frequency, unlike $|F^+_{\rm LR}|$, which vanishes in this case.

IV. CONCLUSIONS

In conclusion, we have considered few-site Kitaev chains and investigated the emergence of superconducting pair correlations. Under general circumstances, we have shown that distinct pair symmetries are allowed to form in these systems as a result of the multiple existing quantum numbers. In the case of a two-site Kitaev chain, we found local pairing with an odd-frequency dependence, while nonlocal pair correlations with both even- and odd-frequency components. While in general the odd-frequency components are linear, we discovered that they acquire a divergent profile around zero frequency in a fine-tuned sweet spot occurring when the parent pair potential and electron tunneling are of the same order and at least one on-site energy tuned to zero. Since these sweet spot regime corresponds to the phase with poor man's Majorana modes, which are fully nonlocal, self-conjugate, and charge neutral, we have interpreted the divergent odd-frequency pairing as a signature of charge neutrality and spatial nonlocality, intrinsic to Majorana quasiparticles. The results presented here can be of use to understand the nature of superconducting correlations in few-site Kitaev chains.

ACKNOWLEDGMENTS

We thank R. Seoane Souto for insightful discussions. We acknowledge financial support from the Swedish Research Council (Vetenskapsrådet Grant No. 2021-04121), the Carl Tryggers Foundation (Grant No. 22: 2093), and the Göran Gustafsson Foundation (Grant No. 2216). The computations were enabled by resources provided by the National Academic Infrastructure for Supercomputing in Sweden (NAISS), partially funded by the Swedish Research Council through Grant Agreement No. 2022-06725.

[1] R. M. Lutchyn, E. P. Bakkers, L. P. Kouwenhoven, P. Krogstrup, C. M. Marcus, and Y. Oreg, Majorana zero modes in superconductor–semiconductor heterostructures, Nat. Rev. Mater. **3**, 52 (2018).

[2] K. Flensberg, F. von Oppen, and A. Stern, Engineered platforms for topological superconductivity and Majorana zero modes, Nat. Rev. Mater. **6**, 944 (2021).

[3] P. Marra, Majorana nanowires for topological quantum computation, J. Appl. Phys. **132**, 231101 (2022).

[4] Y. Tanaka, S. Tamura, and J. Cayao, Theory of Majorana zero modes in unconventional superconductors, Prog. Theor. Exp. Phys. **2024**, 08C105 (2024).

[5] S. D. Sarma, M. Freedman, and C. Nayak, Majorana zero modes and topological quantum computation, npj Quantum Inf. **1**, 15001 (2015).

[6] C. W. J. Beenakker, Search for non-Abelian Majorana braiding statistics in superconductors, SciPost Phys. Lect. Notes, 15 (2020).

[7] R. Aguado and L. P. Kouwenhoven, Majorana qubits for topological quantum computing, Phys. Today **73**(6), 44 (2020).

[8] V. Lahtinen and J. K. Pachos, A short introduction to topological quantum computation, SciPost Phys. **3**, 021 (2017).

[9] A. Y. Kitaev, Unpaired Majorana fermions in quantum wires, Sov. Phys. Usp. **44**, 131 (2001).

[10] A. P. Mackenzie and Y. Maeno, The superconductivity of Sr_2RuO_4 and the physics of spin-triplet pairing, Rev. Mod. Phys. **75**, 657 (2003).

[11] R. M. Lutchyn, J. D. Sau, and S. Das Sarma, Majorana fermions and a topological phase transition in semiconductor-superconductor heterostructures, Phys. Rev. Lett. **105**, 077001 (2010).

[12] Y. Oreg, G. Refael, and F. von Oppen, Helical liquids and Majorana bound states in quantum wires, Phys. Rev. Lett. **105**, 177002 (2010).

[13] E. Prada, P. San-Jose, M. W. de Moor, A. Geresdi, E. J. Lee, J. Klinovaja, D. Loss, J. Nygård, R. Aguado, and L. P. Kouwenhoven, From Andreev to Majorana bound states in hybrid superconductor–semiconductor nanowires, Nat. Rev. Phys. **2**, 575 (2020).

[14] T. Dvir, G. Wang, N. van Loo, C.-X. Liu, G. P. Mazur, A. Bordin, S. L. Ten Haaf, J.-Y. Wang, D. van Driel, F. Zatelli *et al.*, Realization of a minimal Kitaev chain in coupled quantum dots, Nature (London) **614**, 445 (2023).

[15] A. Bordin, X. Li, D. van Driel, J. C. Wolff, Q. Wang, S. L. D. ten Haaf, G. Wang, N. van Loo, L. P. Kouwenhoven, and T. Dvir, Crossed Andreev reflection and elastic co-tunneling in a three-site Kitaev chain nanowire device, arXiv:2306.07696

[16] F. Zatelli, D. van Driel, D. Xu, G. Wang, C.-X. Liu, A. Bordin, B. Roovers, G. P. Mazur, N. van Loo, J. C. Wolff *et al.*, Robust poor man's Majorana zero modes using Yu-Shiba-Rusinov states, arXiv:2311.03193.

[17] S. L. D. ten Haaf, Q. Wang, A. M. Bozkurt, C.-X. Liu, I. Kulesh, P. Kim, D. Xiao, C. Thomas, M. J. Manfra, T. Dvir *et al.*, A two-site Kitaev chain in a two-dimensional electron gas, Nature (London) **630**, 329 (2024).

[18] M. Leijnse and K. Flensberg, Parity qubits and poor man's Majorana bound states in double quantum dots, Phys. Rev. B **86**, 134528 (2012).

[19] J. D. Sau and S. D. Sarma, Realizing a robust practical Majorana chain in a quantum-dot-superconductor linear array, Nat. Commun. **3**, 964 (2012).

[20] R. S. Souto, A. Tsintzis, M. Leijnse, and J. Danon, Probing Majorana localization in minimal Kitaev chains through a quantum dot, Phys. Rev. Res. **5**, 043182 (2023).

[21] R. Seoane Souto and R. Aguado, Subgap states in semiconductor-superconductor devices for quantum technologies: Andreev qubits and minimal Majorana chains, arXiv:2404.06592.

[22] Y. Tanaka, M. Sato, and N. Nagaosa, Symmetry and topology in superconductors–odd-frequency pairing and edge states, J. Phys. Soc. Jpn. **81**, 011013 (2012).

[23] J. Cayao, C. Triola, and A. M. Black-Schaffer, Odd-frequency superconducting pairing in one-dimensional systems, Eur. Phys. J.: Spec. Top. **229**, 545 (2020).

[24] T. Mizushima and K. Machida, Multifaceted properties of Andreev bound states: Interplay of symmetry and topology, Philos. Trans. R. Soc. A **376**, 20150355 (2018).

[25] Y. Asano and Y. Tanaka, Majorana fermions and odd-frequency Cooper pairs in a normal-metal nanowire proximity-coupled to a topological superconductor, Phys. Rev. B **87**, 104513 (2013).

[26] Z. Huang, P. Wölfle, and A. V. Balatsky, Odd-frequency pairing of interacting Majorana fermions, Phys. Rev. B **92**, 121404(R) (2015).

[27] O. Kashuba, B. Sothmann, P. Burset, and B. Trauzettel, Majorana STM as a perfect detector of odd-frequency superconductivity, Phys. Rev. B **95**, 174516 (2017).

[28] S.-P. Lee, R. M. Lutchyn, and J. Maciejko, Odd-frequency superconductivity in a nanowire coupled to Majorana zero modes, Phys. Rev. B **95**, 184506 (2017).

[29] A. Tsintzis, A. M. Black-Schaffer, and J. Cayao, Odd-frequency superconducting pairing in Kitaev-based junctions, Phys. Rev. B **100**, 115433 (2019).

[30] D. Takagi, S. Tamura, and Y. Tanaka, Odd-frequency pairing and proximity effect in Kitaev chain systems including a topological critical point, Phys. Rev. B **101**, 024509 (2020).

[31] S. Tamura, S. Nakosai, A. M. Black-Schaffer, Y. Tanaka, and J. Cayao, Bulk odd-frequency pairing in the superconducting Su-Schrieffer-Heeger model, Phys. Rev. B **101**, 214507 (2020).

[32] D. Kuzmanovski, A. M. Black-Schaffer, and J. Cayao, Suppression of odd-frequency pairing by phase disorder in a nanowire

coupled to Majorana zero modes, Phys. Rev. B **101**, 094506 (2020).
[33] E. Ahmed, S. Tamura, Y. Tanaka, and J. Cayao, Odd-frequency superconducting pairing and multiple Majorana edge modes in driven topological superconductors, arXiv:2404.09517.
[34] J. Cayao and A. M. Black-Schaffer, Odd-frequency superconducting pairing and subgap density of states at the edge of a two-dimensional topological insulator without magnetism, Phys. Rev. B **96**, 155426 (2017).
[35] J. Cayao, P. Dutta, P. Burset, and A. M. Black-Schaffer, Phase-tunable electron transport assisted by odd-frequency Cooper pairs in topological Josephson junctions, Phys. Rev. B **106**, L100502 (2022).
[36] J. Linder and A. V. Balatsky, Odd-frequency superconductivity, Rev. Mod. Phys. **91**, 045005 (2019).
[37] G. D. Mahan, *Many-Particle Physics* (Springer Science & Business Media, New York, 2013).
[38] A. Zagoskin, *Quantum Theory of Many-Body Systems: Techniques and Applications* (Springer, New York, 2014).
[39] M. Sigrist and K. Ueda, Phenomenological theory of unconventional superconductivity, Rev. Mod. Phys. **63**, 239 (1991).
[40] C. Triola, J. Cayao, and A. M. Black-Schaffer, The role of odd-frequency pairing in multiband superconductors, Ann. Phys. **532**, 1900298 (2020).
[41] A. M. Black-Schaffer and A. V. Balatsky, Odd-frequency superconducting pairing in multiband superconductors, Phys. Rev. B **88**, 104514 (2013).
[42] Y. Asano and A. Sasaki, Odd-frequency Cooper pairs in two-band superconductors and their magnetic response, Phys. Rev. B **92**, 224508 (2015).
[43] A. Sasaki, S. Ikegaya, T. Habe, A. A. Golubov, and Y. Asano, Josephson effect in two-band superconductors, Phys. Rev. B **101**, 184501 (2020).
[44] S. Kanasugi, D. Kuzmanovski, A. V. Balatsky, and Y. Yanase, Ferroelectricity-induced multiorbital odd-frequency superconductivity in $SrTiO_3$, Phys. Rev. B **102**, 184506 (2020).
[45] J. Cayao, C. Triola, and A. M. Black-Schaffer, Floquet engineering bulk odd-frequency superconducting pairs, Phys. Rev. B **103**, 104505 (2021).
[46] T. Kuhn, B. Sothmann, and J. Cayao, Floquet engineering Higgs dynamics in time-periodic superconductors, Phys. Rev. B **109**, 134517 (2024).
[47] It is worth noting that the role of the dot index for broadening the emerging superconducting symmetries was studied before, see e.g., Refs. [52–54]. However, none of these previous studies addressed few-site Kitaev chains.
[48] D. M. Pino, R. S. Souto, and R. Aguado, Minimal Kitaev-transmon qubit based on double quantum dots, Phys. Rev. B **109**, 075101 (2024).
[49] S. Datta, *Electronic Transport in Mesoscopic Systems* (Cambridge University Press, Cambridge, 1997).
[50] J. Cayao and R. Aguado, Non-Hermitian minimal Kitaev chains, arXiv:2406.18974.
[51] The opposite signs of the local pair amplitudes (F_{LL} and F_{RR}) have also been reported in the local pair amplitudes of finite topological superconductors with MZMs [4]; in our case, however, no topology is involved. Moreover, the Majorana polarization has also been shown to develop opposite signs at the edges of topological superconductors [55]. This suggests an intriguing relation between odd-frequency pairing and Majorana polarization.
[52] P. Burset, B. Lu, H. Ebisu, Y. Asano, and Y. Tanaka, All-electrical generation and control of odd-frequency *s*-wave cooper pairs in double quantum dots, Phys. Rev. B **93**, 201402(R) (2016).
[53] J. Cayao, P. Burset, and Y. Tanaka, Controllable odd-frequency Cooper pairs in multisuperconductor Josephson junctions, Phys. Rev. B **109**, 205406 (2024).
[54] B. Sothmann, S. Weiss, M. Governale, and J. König, Unconventional superconductivity in double quantum dots, Phys. Rev. B **90**, 220501(R) (2014).
[55] O. A. Awoga and J. Cayao, Identifying trivial and Majorana zero-energy modes using the Majorana polarization, arXiv:2406.11991.